Active disturbance rejection sliding mode control for robot manipulation

Fangli Mou and Dan Wu

Department of Mechanical Engineering, Tsinghua University, Beijing, China

Abstract

Purpose – In recent years, owing to the rapidly increasing labor costs, the demand for robots in daily services and industrial operations has been increased significantly. For further applications and human–robot interaction in an unstructured open environment, fast and accurate tracking and strong disturbance rejection ability are required. However, utilizing a conventional controller can make it difficult for the robot to meet these demands, and when a robot is required to perform at a high-speed and large range of motion, conventional controllers may not perform effectively or even lead to the instability.

Design/methodology/approach – The main idea is to develop the control law by combining the SMC feedback with the ADRC control architecture to improve the robustness and control quality of a conventional SMC controller. The problem is formulated and solved in the framework of ADRC. For better estimation and control performance, a generalized proportional integral observer (GPIO) technique is employed to estimate and compensate for unmodeled dynamics and other unknown time-varying disturbances. And benefiting from the usage of GPIO, a new SMC law can be designed by synthesizing the estimation and its history.

Findings – The employed methodology introduced a significant improvement in handling the uncertainties of the system parameters without compromising the nominal system control quality and intuitiveness of the conventional ADRC design. First, the proposed method combines the advantages of the ADRC and SMC method, which achieved the best tracking performance among these controllers. Second, the proposed controller is sufficiently robust to various disturbances and results in smaller tracking errors. Third, the proposed control method is insensitive to control parameters which indicates a good application potential.

Originality/value – High-performance robot tracking control is the basis for further robot applications in open environments and human–robot interfaces, which require high tracking accuracy and strong disturbance rejection. However, both the varied dynamics of the system and rapidly changing nonlinear coupling characteristic significantly increase the control difficulty. The proposed method gives a new replacement of PID controller in robot systems, which does not require an accurate dynamic system model, is insensitive to control parameters and can perform promisingly for response rapidity and steady-state accuracy, as well as in the presence of strong unknown disturbances.

Keywords Robot, Controller design, Active disturbance rejection control (ADRC), Sliding mode control (SMC)

Paper type Research paper

1. Introduction

In recent years, owing to the rapidly increasing labor costs, the demand for robots in daily services and industrial operations has been increased significantly. The conventional industrial robots have successfully been employed to perform specific tasks in a structured production environment. For further applications and human–robot interaction in an unstructured open environment, fast and accurate tracking and strong disturbance rejection ability are required. This will bring substantial advancement in the present robotics technology (Yu *et al.*, 2016; Lunardini *et al.*, 2016; Lau *et al.*, 2016).

The research on control methods for robots has obtained abundant achievements (Brogardh, 2007; Dinham and Fang, 2014; Yu and Rosen, 2013; Su *et al.*, 2010). However, an actual robot system is restricted to several factors, including system modeling accuracy, environmental uncertainty, parameter identification ability and real-time calculation ability. Therefore, most modern control theory strategies based on the accurate mathematical model of a specific system generally remain in the theoretical design. PID control is still the most common form of controller in the existing robot systems, particularly at the joint control level. PID controllers do not depend on the process model and have a simple control structure that makes the PID control easy to implement. However, utilizing a PID controller can make it difficult for the robot to achieve both significant dynamic and static performance (Lunardini *et al.*, 2016). In addition, when a robot is required to perform at a high-speed and large range of motion, a PID controller may not perform effectively or even lead to the instability of the controlled system (Petit *et al.*, 2015).

Sliding mode control (SMC) has been widely applied to robotic systems because of its robustness to unknown exogenous disturbances, parameter variations and model perturbations (Van *et al.*, 2013; Esmaili and Haron, 2017; Naik *et al.*, 2016). However, to achieve a satisfactory performance, the chattering phenomenon that is usually caused by system disturbance can probably damage the actuator of robotic control systems (Yang *et al.*, 2013). To improve the robustness of conventional SMC, some classical control design tools such as the Riccati approach, LMI-based approach and adaptive approach are utilized in control law design (Kim *et al.*, 2000; Chang, 2009; Choi, 2007; Park *et al.*, 2007; Wen and Cheng, 2008). However, these methods use the assumption that uncertainties are essentially H_2 norm-bounded, which is sometimes unreasonable for practical systems. For the characteristics of robot systems, Wang *et al.* (2019) designed a robust SMC methodology for robotic systems with compliant actuators that employed a generalized proportional integral observer technique to estimate the unknown disturbance. Van *et al.* (2019) developed a control methodology for tracking control of robot manipulators, in which a back-stepping nonsingular fast terminal sliding mode controller was used to improve the robustness. However, these methods were not designed for exclusively joint control, and the relative joint tracking performance has not been studied or presented. The dynamics of robot system consists many unmodeled parts and time-varying disturbances such as the payload effect. These can restrict the control law design and reduce the control performance of the SMC.

Active disturbance rejection control (ADRC) is a disturbance rejection control method based on the error feedback (Han, 2009; Li *et al.*, 2013). The ADRC method does not require an accurate dynamic system model because the extended state observer (ESO) is used to estimate unknown disturbance. Further, the ADRC method can achieve the active compensation for the total disturbance (Freidovich and Khalil, 2006). Only some of the basic system information, such as the order of the system and the control input/output channel, are required for controller design. Recently, the ADRC method has been widely used in many practical applications, such as mechanical systems (Dan and Ken, 2009), processing industries control (Zheng and Gao, 2012), spacecraft systems (Xia *et al.*, 2011) and bionic systems (Martinez-Fonseca *et al.*, 2016; Guerrero-Castellanos *et al.*, 2018). This shows strong robustness and significant potential for engineering applications.

Castaneda *et al.* (2015) used ADRC structure to design an adaptive controller to solve the trajectory tracking problem of a "Delta" parallel robot with model uncertainties. Talole *et al.* (2010) used the linear ADRC method with linear ESO to design a controller for the trajectory tracking control of a flexible-joint robotic system, and the experimental result of a rotary single-link robot was presented to indicate the effectiveness of the ADRC approach. Xue *et al.* (2017) proposed a proportional differential (PD)-based ADRC controller for set-point tracking control of robots, and the experimental results of a 1 DOF rotary manipulator were presented

to demonstrate the effectiveness of the modularized ADRC strategy. Madonski (Madonski *et al.*, 2019) used the ADRC framework and generalized proportional integral observer (GPIO) technique to solve the problem of estimating and suppressing periodic disturbances in robot control. The control scheme was tested on a highly oscillatory 3 DOF torsional plant to demonstrate its effectiveness. Ren *et al.* (2018) used the ESO to develop a collision detection method based on ontology sensors (encoder and torque sensor) for a collaborative robot. Dong *et al.* (2020) used ADRC and ESO to design a cascaded torque controller to solve the compliance control problem of joint torque. The authors have proposed an efficient and simple robot controller based on the ADRC method to achieve rapid and stable robot trajectory tracking (MOU *et al.*, 2020). These studies show the application potential of the ADRC method in robot control. However, the conventional ADRC uses the PD feedback law and ESO for disturbance suppression, which suffers the same problems as a PID controller when the disturbance cannot be totally observed (Madonski *et al.*, 2019). This observation error and related effect are unavoidable in real robot applications, and it becomes difficult to improve the control performance of ADRC. For robot controllers that require high speed and significant precision with various kinds of disturbance, it is difficult for simple PID-based feedback law to achieve satisfactory results under several conditions.

In this study, a practical and effective robot trajectory tracking control method is developed based on the ADRC framework. This provides both fast response and high accuracy in the nominal as well as in the systems with unknown uncertainties and time-varying disturbances. The main idea is to develop the control law by combining the SMC feedback with the ADRC control architecture to improve the robustness and control quality of a conventional SMC controller. First, a tracking differentiator is used to process the reference trajectory to obtain the smoothed continuous reference trajectory and its derivatives. To estimate the model uncertainties and unknown time-varying disturbances, the GPIO technique is employed to design the control law. As compared with ESO, the GPIO can significantly eliminate the disturbance in the polynomial form, which commonly exists in the robot system. With the help of GPIO, the new SMC feedback law can be designed for disturbance suppression and high tracking accuracy. In addition, the robustness of the robot system is further improved. A simulation example of a manipulator tracking control under different test conditions is provided to demonstrate the effectiveness and advantage of the proposed control strategy.

In summary, the main contributions of this paper are as follows. (1) A novel observer-based SMC method is proposed for robot control. (2) The design procedure is practical and robust to model uncertainties. (3) The selected sliding surface and ADRC framework can achieve a fast transient response, low steady state error and strong disturbance rejection ability. (4) In comparison with other state-of-the-art methods, such as PID, conventional SMC and ADRC, the proposed approach provides a superior performance.

The remainder of this paper is organized as follows. A brief introduction to the dynamic model of a robot is given in Section 2. The design of the proposed active disturbance rejection SMC is presented in Section 3. The numerical simulation results in Section 4 demonstrate the effectiveness of the proposed control method by comparing it with the other three control methods under different test conditions. Finally, conclusions are presented in Section 5.

2. Modeling of robot system

Figure 1 shows the robot model considered in this study, which consists of a manipulator composed of n links connected by n single-degree-of-freedom joints. F_b is the base frame, which remains the same in our study; q_i is the i-th joint angle; g is the gravity vector.

Based on the Euler–Lagrangian method, the dynamic model of an n-joint robot manipulator is usually expressed in joint space coordinates as follows (Khatib and Burdick, 1986):
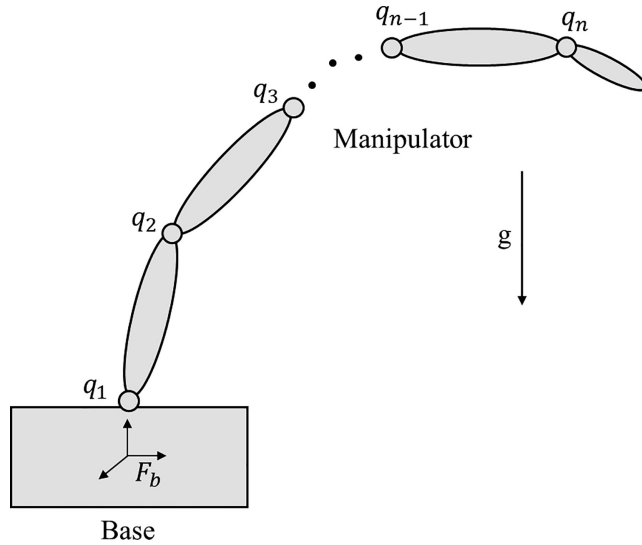
Figure 1.
Model of an n-DOF
robot manipulator

$$D(q)\ddot{q} + C(q, \dot{q})\dot{q} + G(q) + d(q, \dot{q}, \ddot{q}, t) = \tau, \qquad (1)$$

where $q, \dot{q}, \ddot{q} \in R^{n \times 1}$ denote the joint position, velocity and acceleration, respectively; $\tau \in R^{n \times 1}$ is the joint torque; $D(q) \in R^{n \times n}$ is the symmetric positive definite inertia matrix; $C(q, \dot{q}) \in R^{n \times n}$ includes the nonlinear Coriolis and centrifugal forces acting on the system; $G(q) \in R^{n \times 1}$ is the term of gravitational torque and $d(q, \dot{q}, \ddot{q}, t) \in R^{n \times 1}$ is the generalized system disturbance that contains unmodeled system dynamics and external disturbance.

By defining the variables as $x_1 = q$, $u = \tau$, $y = x_1$, the system dynamics (1) can be presented as the following state-space description:

$$\begin{cases} \dot{x}_1 = x_2 \\ \dot{x}_2 = D^{-1}(x_1) \cdot (-C(x_1, x_2)x_2 - G(x_1) - d + u) \\ y = x_1 \end{cases} \qquad (2)$$

3. Design of robot controller

In this section, we present a trajectory tracking controller using the ADRC architecture. The customized SMC law is designed for the basic tracking performance. Thus, a GPIO is employed to obtain and compensate the generalized system disturbance. The structure of the proposed control strategy is illustrated in Figure 2.
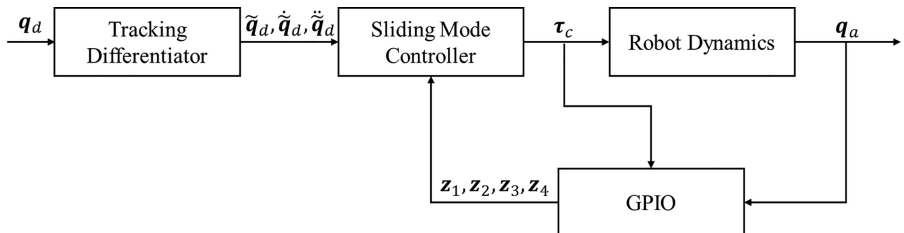

Figure 2.
Control structure of the
proposed control
framework

In Figure 2, q_d is the desired trajectory, $\tilde{q}_d$, $\dot{\tilde{q}}_d$, $\ddot{\tilde{q}}_d$ represents the smoothed q_d and its derivatives, respectively, τ_c is the control torque, q_a is the actual joint state and z_1, z_2, z_3, z_4 are the estimation of system states and disturbances.

3.1 Proposed control structure

The control objective for the considered trajectory tracking is to achieve high control accuracy and strong control robustness. The desired trajectory in practice usually has only position information and discontinuity point, thus requiring to carry out preprocessing for further design.

The tracking differentiator (TD) (Han, 2009) is an efficient component to obtain the smooth desired signal and its derivatives from the provided position signal, which can be expressed in the following form:

$$
\begin{cases}
q_1 = q_1 + h \cdot q_2 \\
q_2 = q_2 + h \cdot \text{fhan}(q_1 - q_d, c_1 q_2, r_0, h) \\
q_3 = q_3 + h \cdot \text{fhan}(q_3 - q_2, c_2 q_3, r_1, h)
\end{cases}
\tag{3}
$$

where $q_i = \tilde{q}_d^{(i)}$ are the generated reference trajectories from the given signal, h is the controller instruction cycle,and $\text{fhan}(x_1, cx_2, r_0, h_0)$ is a nonlinear function represented as follows:

$$
\begin{cases}
d = r_0 h_0^2, \ a_0 = h_0 c x_2, \ y = x_1 + a_0 \\
a_1 = \sqrt{d(d + 8|y|)} \\
a_2 = a_0 + \text{sgn}(y)(a_1 - d)/2 \\
s_1 = (\text{sgn}(y + d) - \text{sgn}(y - d))/2 \\
a = (a_0 + y - a_2)s_1 + a_2 \\
s_2 = (\text{sgn}(a + d) - \text{sgn}(a - d))/2 \\
\text{fhan}(x_1, cx_2, r_0, h_0) = -r_0(a/d - \text{sgn}(a))s_2 - r_0 \text{sgn}(a)
\end{cases}
\tag{4}
$$

The parameter r_0 affects the tracking rapidity of TD. The parameter h_0 is the speed factor to eliminate high frequency output oscillations, which is usually set larger than the controller instruction cycle h, and c is the damping factor that determines the dynamic characteristic of the TD's transient tracking process.

The ADRC scheme uses the state observer to compensate for the total disturbance that can influence the system output. For robot system (2), the total disturbance can be defined as

$$
f_{ob} = D^{-1}(-C'(x_1, x_2)x_2 - G'(x_1) - d)
\tag{5}
$$

where $C'(x_1, x_2)$ and $G'(x_1)$ represent the system model error of $C(x_1, x_2)$ and $G(x_1)$, respectively.

Based on the disturbance observer, the observed total disturbance f_{ob} can be used as an additional state x_3, and the control torques can be designed as

$$
\tau_c = \tau_0 - D x_3
\tag{6}
$$

where τ_0 is the control torque generated by the feedback control law, which is usually designed based on the corresponding integrating system.

The conventional ADRC uses an ESO to obtain the total disturbance (Han, 2009). The ESO-based controller can significantly eliminate the total disturbance with a constant or gradually varying form using a simple PD-controller. Other types of total disturbance can

have the bounded estimation errors under the assumption that f_{ob} is bounded or its time derivative is bounded (Zhou *et al.*, 2009).

The total disturbance can be expressed by the following Taylor polynomials (Wang *et al.*, 2016) assuming the first m time derivatives of f_{ob} exist,

$$f_{ob} = \sum_{i=0}^{m-1} \alpha_i t^i \tag{7}$$

where, $\alpha_i = \text{diag}(\alpha_{i1}, a_{i2}, \ldots, a_{in})$, and $\alpha_{i1}, a_{i2}, \ldots, a_{in}$ are unknown constant coefficients.

The GPIO (Sira-Ramirez *et al.*, 2018), which can be considered as a corresponding higher-order version of ESO, is used to estimate unknown time-varying disturbances f_{ob}. Suppose system output is $y = q$, and $x_{i+3} = f_{ob}^{(i)}$, $(i \geq 1)$, the GPIO with the chosen order $m > 1$ can be derived as

$$\begin{cases} e = z_1 - y \\ \dot{z}_1 = z_2 - \beta_1 \cdot e \\ \dot{z}_2 = z_3 - \beta_2 \cdot e + b_0 \cdot u \\ \dot{z}_{i+2} = z_{i+3} - \beta_{i+2} \cdot e \\ i = 1, 2, \ldots m - 1 \\ \dot{z}_{m+3} = -\beta_{m+3} \cdot e \end{cases} \tag{8}$$

where $z_1, z_2, \ldots, z_{m+3}$ are the estimations of $x_1, x_2, \ldots, x_{m+3}$, respectively, $\beta_i = \text{diag}(\beta_{11}^i, \beta_{22}^i, \ldots, \beta_{nn}^i)$, $\beta_{11}^i, \beta_{22}^i, \ldots, \beta_{mm}^i > 0$ are the observer gains, b_0 is the estimated value of D^{-1}, and u is the control torque.

Using the similar compensation law (7), the GPIO can significantly eliminate up to m-order polynomials from the total disturbance because the disturbance estimation of GPIO (8) can track the disturbance $f_{ob}^{(i)}$ asymptotically. That implies,

$$\lim_{t \to \infty} (z_i - x_i) = 0, \, i = 1, 2, \ldots m \tag{9}$$

The estimation-error state matrix of GPIO (9) has the following form:

$$H_G = \begin{bmatrix} -\beta_{nn}^1 & 1 & 0 & \ldots & 0 \\ -\beta_{nn}^2 & 0 & 1 & & \vdots \\ -\beta_{nn}^3 & & & \ddots & 0 \\ \vdots & \vdots & & & 1 \\ -\beta_{nn}^{m+3} & 0 & & \ldots & 0 \end{bmatrix} \tag{10}$$

Following the pole-placement controller tuning methodology from (Gao, 2003), the observer gains can be selected by matching a desired stable polynomial $P_o(s) = (s + \omega_o)^{m+3}$, where $\omega_o = [\omega_{o1}, \omega_{o2}, \ldots, \omega_{on}]^T$ represents the observer bandwidth, which is selected as a design parameter. With the pole-placement approach, the observer gains are selected as

$$P_o(s) = \det(sI - H_G) \tag{11}$$

As a result, we can select the GPIO gains as

$$\beta_i = C_{m+3}^i \omega_o^i, \quad i = 1, 2, \ldots m \tag{12}$$

Generally, to obtain higher observer accuracy and improved closed-loop performance, a higher-order m should be selected. However, it should be noted that increasing the number of

extended states m in GPIO indicates the use of a higher observer bandwidth. Consequently, the GPIO from (8) could be more sensitive to measurement noise and will increase the computational effort significantly, which can cause performance degradation or even oscillation. Therefore, a balanced condition should be achieved among the observer accuracy, the measurement noise and the system computational ability (Sun *et al.*, 2016).

For the robot system, mechanical structures and actual application usually cause relatively smooth disturbances, and thus the disturbance, which can be expressed as (7) by setting the order $m = 1$, is a very common case and can be a significant fraction of the joint torque when the robot runs. In the particular case considered in this study, only one extended state ($m = 1$) is used to estimate the total disturbance.

3.2 Control loop design
As the GPIO output z_{i+3} is the estimation of the disturbance $f_{ob}^{(i)}$ for $i \geq 0$, to develop control law (6), the GPIO-based SMC law is designed to achieve tracking performance. For a practical robot, only the joint position is measurable accurately, based on the encoder information. Hence, the sliding-mode surface s for robot system (1) is given by

$$s = c_1 e_1 + e_2 \tag{13}$$

where $e_1 = q_d - q_a$, and $e_2 = \dot{q}_d - \dot{q}_a$ represent the joint tracking errors; $c_1 = \text{diag}(c_{11}, c_{12}, \ldots, c_{1n})$, $c_{11}, c_{12}, \ldots, c_{1n}$ are the constant sliding mode surface parameters and $c_{11}, c_{12}, \ldots, c_{1n} > 0$.

Subsequently, the approach law can be represented as

$$\dot{s} = -\xi \text{sgn}(s) - ks \tag{14}$$

where $\xi = \text{diag}(\xi_1, \xi_2, \ldots, \xi_n)$, $\xi_1, \xi_2, \ldots, \xi_n > 0$ and $k = \text{diag}(k_1, k_2, \ldots, k_n)$, $k_1, k_2, \ldots, k_n > 0$.

Combining (1) and (8), the GPIO-based SMC law is represented as

$$\begin{aligned} \tau_c &= D(c_1 \dot{e}_1 + \ddot{q}_d + \xi \text{sgn}(s) + ks) \\ &+ C_0(q, \dot{q})\dot{q} + G_0(q) - Df(z_4)z_3 + f_c \end{aligned} \tag{15}$$

where $C_0(q, \dot{q})$ and $G_0(q)$ are the nominal system models of $C(q, \dot{q})$ and $G(q)$; $f(z_4)$ is the adaptive regularization term to avoid a rapid change in compensation; f_c is the estimate bound of system error selected as

$$f_c = D((\sigma_3 + f_u) \odot \text{sgn}(s) - f_l) \tag{16}$$

where $\odot$ is the Hadamard product operator, which represents the elementwise product of two matrices; σ_3 is the bound of $|z_3 - x_3|$; f_u and f_l and f_l are the upper bound and lower bound estimates of initial states, and hence $f_u \geq f_l$. The larger f_c can cause significantly higher chatter when defined errors e_1 and e_2 approach near the sliding surface $s = 0$; to obtain better control quality, we can provide some decay factors $\zeta_i(t)$ to revise the estimated f_c as

$$f_c' = D((\zeta_1(t)\sigma_3 + \zeta_2(t)f_u) \odot \text{sgn}(s) - \zeta_3(t)f_l) \tag{17}$$

where $\zeta_1(t)$ is monotonically decreasing, and $\zeta_2(t)$, $\zeta_3(t)$ can be selected as the piecewise function that $\zeta_2(t)$, $\zeta_3(t) = 0$ when $t \geq t_0$, t_0 is given time.

As we set the observer order $m = 1$ in GPIO (9), the estimation errors of GPIO can rapidly converge to 0 when z_4 changes gradually, which means the total disturbance does not change faster than the ramping function. In contrast, estimation errors will increase when z_4 has a relatively large value.

Evidently, large estimation errors will affect the closed-loop performance. To increase the control robustness, we use $z_4(t) = [z_{41}, z_{42}, \ldots, z_{4n}]^T$ to regularize the compensation term

from GPIO. The Gaussian functions $\varphi_i(z_{4i})$ are used to perform the weighting transformation as

$$\varphi_i(z_{4i}) = \exp\left(-z_{4i}^2/\sigma_i^2\right) \tag{18}$$

where σ_i is the compensation variance for each joint; large σ_i means the corresponding estimation is substantially reliable.

The time profile of $z_4(t)$ is introduced to perform time-domain weighting,

$$\gamma_i(t - t_f) = \begin{cases} 0, & t < t_f \\ 1 - e^{-a_i\left(t - t_f\right)}, & t > t_f \end{cases} \tag{19}$$

where a_i represents the disturbance evolution rate; large a_i means the disturbance has weak time-correlation and t_f is the weighting time length.

Combining (19) and (20), the regularization term $f(z_4)$ can be derived as

$$f(z_4(t)) = \text{diag}(f_1(z_{41}(t)), f_2(z_{42}(t)), \ldots, f_n(z_{4n}(t)))f_i(z_{4i}(t))$$

$$= \frac{1}{t_f} \int_0^t \gamma_i(\tau - t_f)\varphi_i(z_{4i}(\tau))d\tau \tag{20}$$

Summarizing the above analysis, the proposed DOSMC (disturbance observer sliding mode control) method, illustrated in Figure 2, can finally be obtained.

3.3 Stability analysis
Proof: Combining (14) and (16), the derivative of sliding surface (14) can be modified as follows:

$$\dot{s} = c_1\dot{e_1} + \dot{e_2} = c_1\dot{e_1} + \ddot{q}_d - \ddot{q}_a$$

$$= c_1\dot{e_1} + \ddot{q}_d - D^{-1}(-C(x_1, x_2)x_2 - G(\mathbf{x}_1) - d) - D^{-1}\tau_c$$

$$= -D^{-1}(-C(x_1, x_2)x_2 - G(x_1) - d - C_0(x_1, x_2)x_2) - D^{-1}(G_0(x_1) + f_c) - \xi\text{sgn}(s)$$

$$\quad - ks + f(z_4)z_3 \tag{21}$$

According to the defined additional state x_3 and GPIO (8), we can have

$$\dot{s} = -D^{-1}(-C^{'}(x_1, x_2)x_2 - G^{'}(x_1) - d + f_c) - \xi\text{sgn}(s) - ks + f(z_4)z_3$$

$$= -\xi\text{sgn}(s) - ks - D^{-1}f_c - x_3 + f(z_4)z_3 \tag{22}$$

$$= -\xi\text{sgn}(s) - ks - D^{-1}f_c + \eta_3 + (f(z_4) - I)z_3$$

where $\eta_3 = z_3 - x_3$ is the estimation error of GPIO that is bounded under the assumption that f_{ob} is bounded.

Consider the following Lyapunov function:

$$V(s) = \frac{1}{2}s^T s \tag{23}$$

The derivative of $V(s)$ yields

$$
\begin{aligned}
\dot{V}(s) = s^T \dot{s} \quad &= s^T\left(-\xi \mathrm{sgn}(s) - ks - D^{-1}f_c + \eta_3\right) \quad + s^T((f(z_4) - I)z_3) \\
&= -\sum_{i=1}^{n} \xi_i |s_i| - \sum_{i=1}^{n} k_i s_i^2 - \sum_{i=1}^{n} |s_i|((\sigma_3 + f_u)_i) + s^T(f_l + \eta_3 + (f(z_4) - I)z_3) \\
&\leq -\sum_{i=1}^{n} \xi_i |s_i| - \sum_{i=1}^{n} k_i s_i^2 - \sum_{i=1}^{n} |s_i|((\sigma_3 + f_u)_i) + \sum_{i=1}^{n} |s_i|(|(f_l)_i| + |(\eta_3)_i| + |(z_3)_i|) \\
&\leq -\sum_{i=1}^{n} \xi_i |s_i| - \sum_{i=1}^{n} k_i s_i^2 \leq 0
\end{aligned}
\tag{24}
$$

This means that the defined errors e_1, e_2 arrive at the sliding surface $s = 0$ in finite time. The sliding motion is then described as

$$
c_1 e_1 + e_2 = 0
\tag{25}
$$

Since $c_1 > 0$, system (22) can be verified to be exponentially stable. This shows that the tracking error will slide to the equilibrium point asymptotically under the proposed DOSMC control law. This completes the proof.

4. Numerical simulations and comparative analysis
In this section, a simulation example of a 6 DOF robot is presented to demonstrate the effectiveness of the proposed control method. The structure of robot is as shown in Figure 3.

Figure 3.
Structure of the simulation 6 DOF robot

The proposed DOSMC method was compared with the PID controller, conventional SMC method and LADRC (linear active disturbance rejection control) method. In the following examples, all the controller frequencies are set up to 1 kHz. The coupling effect of other joints is reflected in the applied disturbance torque.

4.1 Simulation example

The tracking process was simulated in a MATLAB/ Simulink environment. The block diagram of the simulation system is shown in Figure 4. The manipulator is a rigid-link rigid-joint mechanism, which is set up using the MATLAB/ SimMechanics toolbox. The robot parameters are set as the design values of real robot as seen in Figure 3.

The motor and driver dynamics are modeled as a double mass spring damping system, which can be seen from Eqn (27). The disturbance applied to both ends of the link and the torque side for different simulation cases. The add noise channel block provides band-limited white noise to reflect the system measurement noise with different levels of signal-to-noise ratio (SNR) in the corresponding channels.

The motor and driver model is described as

$$T_L = \frac{J_L}{J_L + J_M} \cdot \frac{b_s s + K_s}{J_p s^2 + b_s s + K_s} T_E$$

$$J_p = \frac{J_M J_L}{J_L + J_M}$$

(26)

where J_M, J_L represents the motor inertia and motor load inertia, respectively, b_s represents the transmission damping and K_s represents the transmission stiffness. In the simulation, these parameters are selected as $J_M = 1.88 \times 10^{-3}(kg \cdot m^2)$, ... $J_L = 3.13 \times 10^{-3}(kg \cdot m^2)$, $b_s = 1.88 \times 10^{-3}(Nm/s)$ and $K_s = 3.78 \times 10^6(N/m)$.

The design and performance of the disturbance observer can be affected by the measurement noise. To simulate noise in actual measurements, we analyzed the data collected from a practical robot. The SNR of the position and velocity channel is approximately 124 dB and 74 dB, respectively. A comparison of the simulation and experimental measurements is shown in Figure 5. As can be seen in Figure 5, the add noise channel block can provide the measurement noise with high model accuracy which represents the simulation results more reasonably.
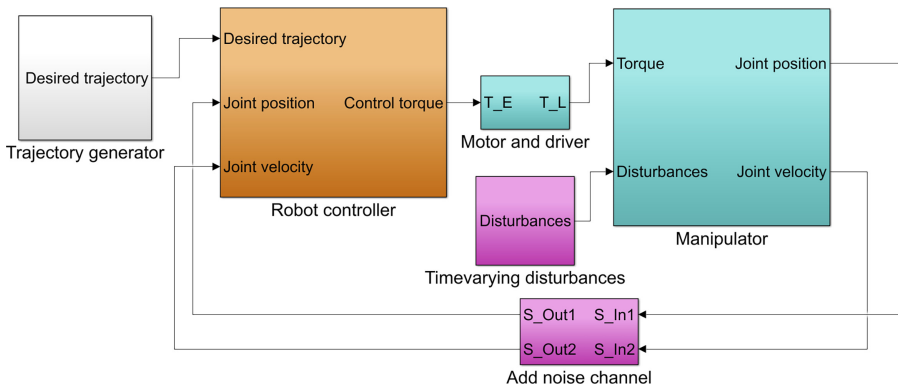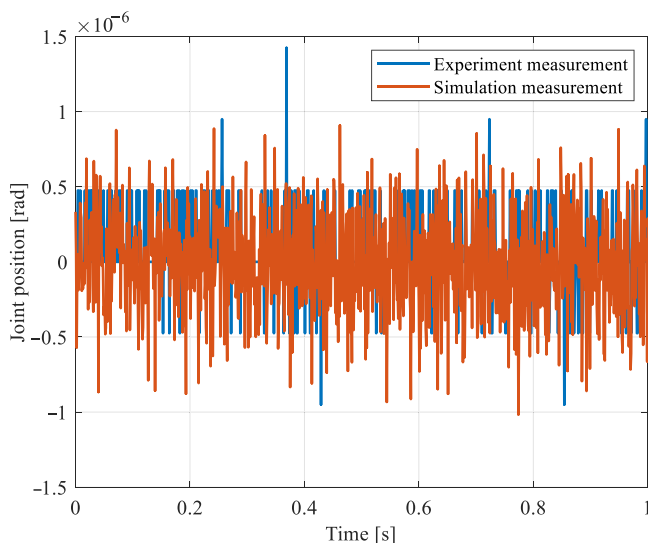

Figure 4.
Block diagram of the simulation robot system

Figure 5.
Position measurement
in simulation and
experiment

4.2 Simulation results and discussion

Firstly, we tested the GPIO loop with different noise levels, and the PD controller is used as the feedback controller. Figure 6 shows the corresponding tracking performance. It is evident that the used GPIO loop can be stable when the measurement SNR is larger than 40 dB, which can be sufficiently satisfied in our robot system.

In the first simulation case, no disturbances were applied to the robot system, and the tracking performance of the nominal system was tested. The joint friction is modeled as the following Coulomb viscous friction:

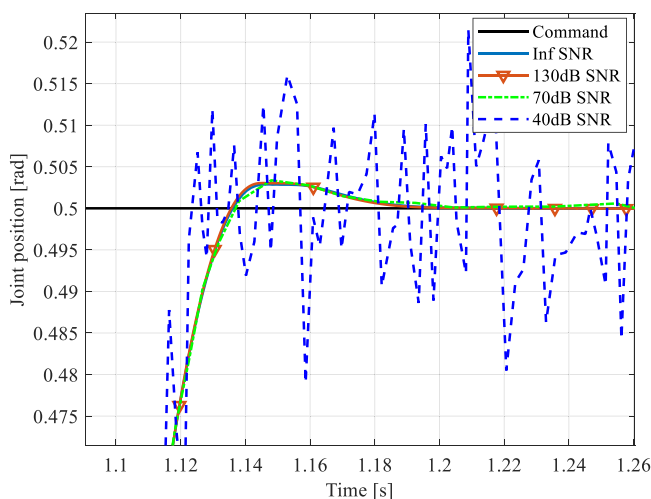$$\tau_{f,n} = f_{c1}\mathrm{sgn}(\dot{q}_n) + f_{c2}\dot{q}_n \qquad (27)$$

Figure 6.
The GPIO performance
under different
measurement noises

The friction parameters of each joint in Eqn (27) are set according to the system dynamic identification results:

$$f_{c1} = [5.6665, 2.951, 2.7750, 2.9656, 1.4458, 1.5185],$$
$$f_{c2} = [10.4242, 13.1298, 9.6565, 3.5454, 2.4864, 2.0506],$$

In this case, the sliding friction is almost completely compensated (approximately 90%) by the feedforward law. For comparison, the first observer gain of the GPIO and ESO is selected to have the same value of 800. According to the robot manual, the joint torques are limited to corresponding rated torques of 85 Nm, 85 Nm, 30 Nm, 30 Nm, 10 Nm, and 10 Nm.

The square waves were set as the reference joint torque signals. The tracking performance comparisons of the abovementioned controllers are demonstrated in Figure 7. All the controller parameters are optimized using the particle swarm optimization, and the control objective function is developed by investigating the dynamic performance and stable error, to achieve balanced performance on response rapidity and steady-state error while keeping the system stable. All these controller parameters remain the same in the following simulation cases.

Figure 8 shows the tracking responses of joint 3. The amplitude of the reference square wave and sine wave is 57.29 °, which is considered as a large moving range in practice. As can be seen in Figure 8, the proposed DOSMC law can achieve excellent tracking performance for both response rapidity and steady-state accuracy under different forms of reference input.

More specifically, four representative step-response characteristics were selected to compare the robot tracking performance under these controllers. Table 1 shows the calculation results, where t_r, M_p, t_s, e_{ss} represents the average rise time of 90% steady-state, overshoot percentages, settling time within the 1% error band and steady-state error, respectively.

It can be observed that the conventional PID controller cannot balance the response rapidity and steady-state accuracy, which has a significant overshoot and largest steady-state error. Owing to the estimation of ESO, the LADRC method can significantly reduce the overshoot. However, since the feedback law of LADRC is a PD controller, the steady-state error is difficult to further decrease and settling time is longer. The SMC method designed the sliding motion to improve control performance, which decreases the steady-state error. The ADRC scheme can provide the estimation of the total disturbance, which reduces the impact of perturbation. The proposed DOSMC method combines the advantages of the ADRC and SMC method, which achieved the best tracking performance among these controllers, greatly decreases the steady-state error and increases the time required to reach a steady state. Therefore, it is proved that the control method, proposed in this paper, achieves a good performance on a nominal system.

For a practical robot system, an unknown time-varying disturbance is applied every time. In addition, the system dynamics cannot be modeled accurately. In the following simulation cases, different types of disturbances are applied to the system to analyze the controller robustness. As can be seen in Figure 7, due to the structure of robot, the joint 3 usually works under the condition that controllers have the worst performance. For clearly demonstrating, we only give the performance of joint 3 in the following discussion.

The total disturbance d_w comprises of three parts: the external disturbance d_1, the payload changing term d_2 and the modeling error d_3. The external disturbance d_1 is considered in the following form:

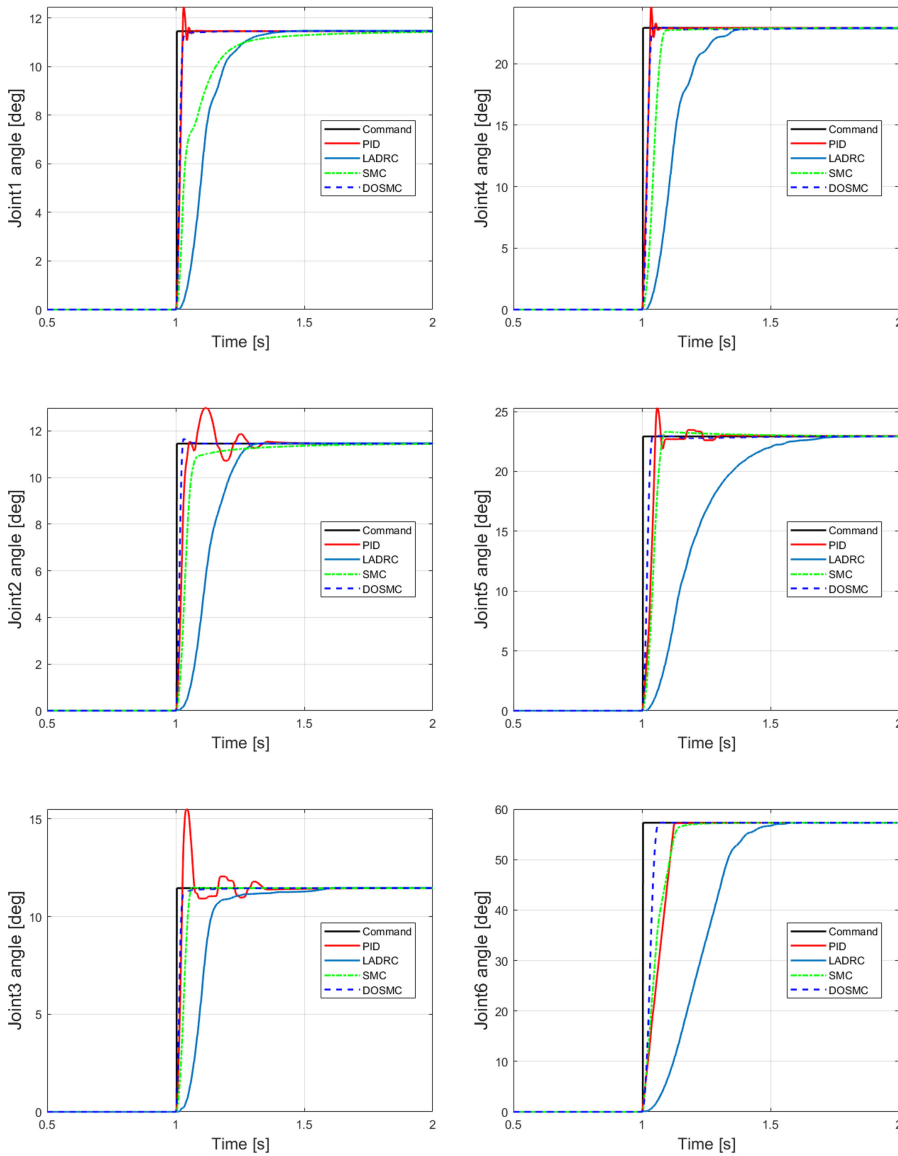$$d_1 = \begin{cases} 0, & t < t_0 \\ A_0\sin(8\pi(t - t_0)) + A_1\text{tri}(t - t_1) + A_2, & t \geq t_0 \end{cases} \tag{28}$$

Figure 7.
System tracking
responses of
comparative methods

where tri(t) is the unit triangle wave with 0.25 Hz, and the maximum amplitude of d_1 is 15 Nm, which is 50% of the motor nominal torque.

The payload changing term d_2 is given as follows: when $t < t_2$, no load is applied; when $t \geq t_2$, a payload of 2 kg is carried by the robot.

The reference trajectory is a step signal (5.73°) and a sine wave (5.73° and 1 Hz). The modeling error d_3 contains the complete joint friction, which implies that no feedforward torque is applied. The simulation results are shown in Figure 9.
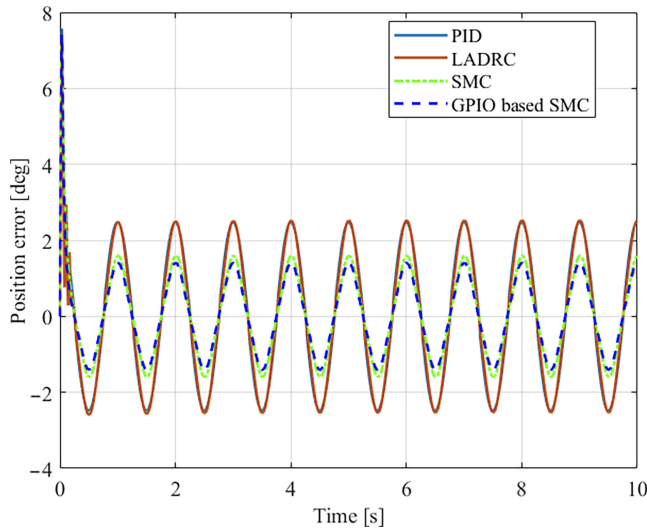
|	PID	LADRC	SMC	DOSMC
tr [ms]	46.67	246.41	80.16	30.33
Mp	12.54%	0%	0.27%	0.26%
ts [ms]	252.54	457.16	254.67	45.58
ess [deg]	0.031	0.014	0.0055	0.00018

It can be clearly observed that the proposed DOSMC law can significantly suppress the influence of the applied time-varying disturbance regardless of the cause such as changing payload or external disturbance. More specifically, for steady state, the maximum tracking error of the PID controller, LADRC method, SMC method and proposed DOSMC method are 1.43 °, 0.65 °, 0.054 ° and 0.011 °, respectively. The GPIO loop can provide stronger estimation and compensation of unknown disturbances, particularly the ramping form. This indicates that the controller is sufficiently robust to various disturbances and results in smaller tracking errors. This case proves that the proposed control method in this study has good application potential.

For the observer-based control law (7), the system parameter D is important to the control performance and requires more accurate prior estimation. However, in an actual robot system, D varies significantly during the motion of the robot, and the exact value is difficult to obtain. Finally, in the third simulation case, we tested the performance of the proposed control method for a large estimation error of the system parameter D.

Figure 10 shows the tracking performance of the LADRC and the proposed DOSMC method, where the same form of disturbance in the previous simulation is applied. As can be seen in Figure 8, the estimation system parameter b varies from 0.1 times to 10 times the nominal value b_0. Owing to the customized SMC law, the maximum tracking trajectory variation of the proposed DOSMC method is approximately 0.1°, while that of LADRC is approximately 4.5°. It is evidently observed that the simulation results validated the robustness of the control toward the system parameter D. This indicates that the proposed control method is insensitive to control parameters and has a good application potential.
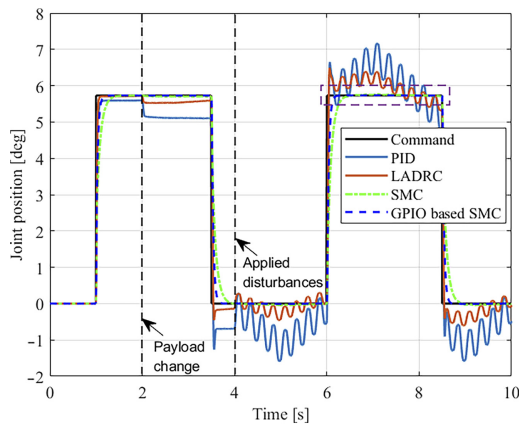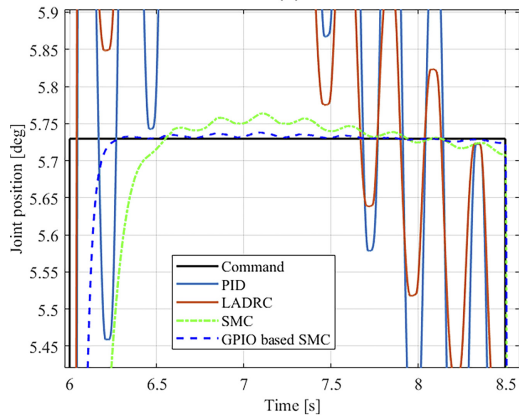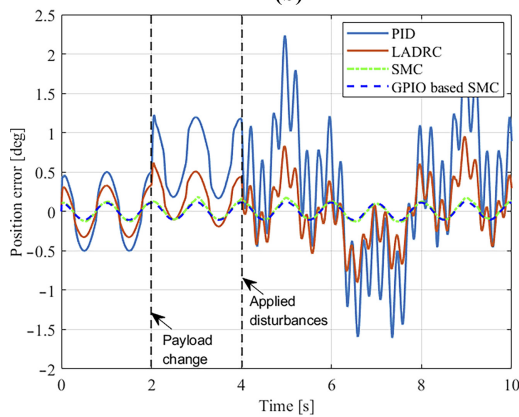
Figure 9.
System tracking
responses of the
comparative methods
in the presence of an
unknown time-varying
disturbance (a) Joint
position under the four
control methods to
square wave reference
input. (b) The local
enlargement of the
dashed box in (a). (c)
Trajectory tracking
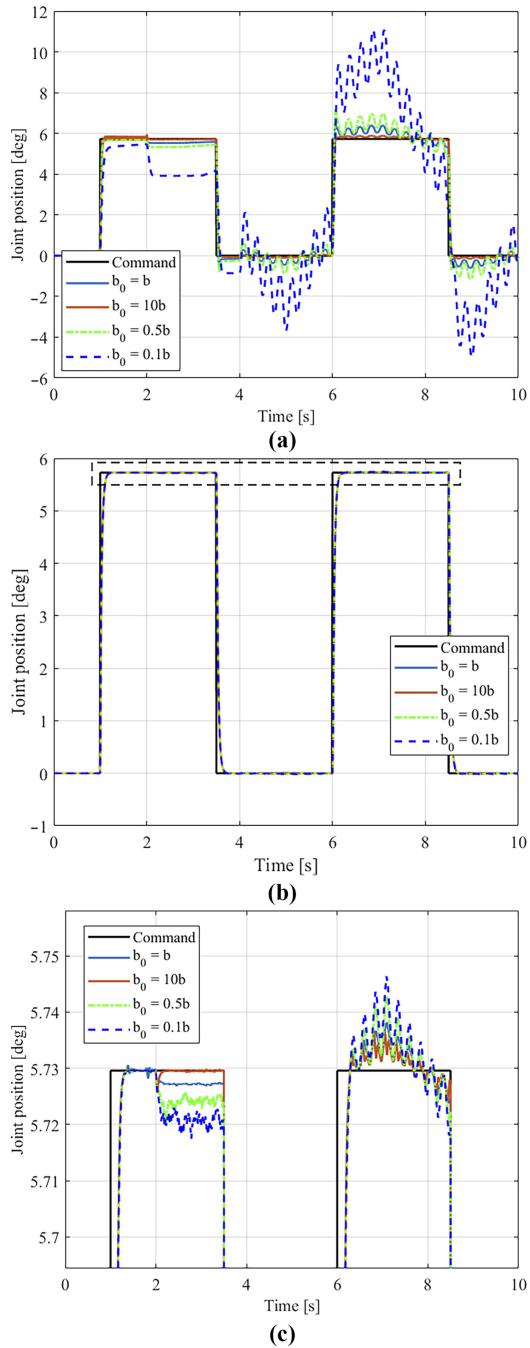errors for the sine wave
reference

Figure 10.
System tracking
responses of the
comparative methods.
(a) Joint position under
the LADRC method to
square wave reference
input. (b) Joint position
under the proposed
control method. (c) The
local enlargement of
the dashed box in (b)

5. Conclusions

The reference trajectory tracking problem for robots, subjected to unknown uncertainties and time-varying disturbances, is studied in this study. By using the ADRC structure, the active disturbance rejection SMC is designed based on the GPIO technique that can achieve high tracking rapidity and accuracy while simultaneously considering the time-varying disturbances. The employed methodology introduced a significant improvement in handling the uncertainties of the system parameters without compromising the nominal system control quality and intuitiveness of the conventional ADRC design. The simulation results of three test cases verified that the proposed control method can achieve a satisfactory tracking performance and has significant practical application potential. Future work is to improve the optimal design of control parameters and to study the control effect of the practical controller under specific work tasks.

References

Brogardh, T. (2007), "Present and future robot control development—an industrial perspective", *Annual Review in Control*, Vol. 31 No. 1, pp. 69-79.

Castaneda, L.A., Luviano-Juarez, A. and Chairez, I. (2015), "Robust trajectory tracking of a delta robot through adaptive active disturbance rejection control", *IEEE Transactions on Control Systems Technology*, Vol. 23 No. 4, pp. 1387-1398, doi: 10.1109/tcst.2014.2367313.

Chang, J.-L. (2009), "Dynamic output integral sliding-mode control with disturbance attenuation", *IEEE Transactions on Automatic Control*, Vol. 54 No. 11, pp. 2653-2658.

Choi, H.H. (2007), "LMI-based sliding surface design for integral sliding model control of mismatched uncertain systems", *IEEE Transactions on Automatic Control*, Vol. 52 No. 4, pp. 736-742.

Dan, W. and Ken, C. (2009), "Design and analysis of precision active disturbance rejection control for noncircular turning process", *IEEE Transactions on Industrial Electronics*, Vol. 56 No. 7, pp. 2746-2753, doi: 10.1109/tie.2009.2019774.

Dinham, M. and Fang, G. (2014), "Detection of fillet weld joints using an adaptive line growing algorithm for robotic arc welding", *Robotics and Computer-Integrated Manufacturing*, Vol. 30 No. 3, pp. 229-243.

Dong, Y.F., Ren, T.Y., Wu, D. and Chen, K. (2020), "Compliance control for robot manipulation in contact with a varied environment based on a new joint torque controller", *Journal of Intelligent and Robotic Systems*, Vol. 12, doi: 10.1007/s10846-019-01109-8.

Esmaili, P. and Haron, H. (2017), "Adaptive neuro integral sliding mode control on synchronization of two robot manipulators[C]", *Conference on Computational Collective Intelligence Technologies and Applications*, Springer, Cham.

Freidovich, L.B. and Khalil, H.K. (2006), "Robust feedback linearization using extended high-gain observers", *Proceedings of IEEE Conference on Decision and Control San Diego*, California, CA, pp. 983-988.

Gao, Z. (2003), "Scaling and bandwidth-parameterization based controller tuning", *In American Control Conference*, Vol. 6, pp. 4989-4996.

Guerrero-Castellanos, J.F., Rifai, H., Arnez-Paniagua, V., Linares-Flores, J., Saynes-Torres, L. and Mohammed, S. (2018), "Robust active disturbance rejection control via control Lyapunov functions: application to actuated-ankle-foot-orthosis", *Control Engineering Practice*, Vol. 80, pp. 49-60.

Han, J. (2009), "From PID to active disturbance rejection control", *IEEE Transactions on Industrial Electronics*, Vol. 56 No. 3, pp. 900-906.

Khatib, O. and Burdick, J. (19861986), "Motion and force control of robot manipulators", *Proceedings. 1986 IEEE International Conference on Robotics and Automation*, pp. 1381-1386.

Kim, K.S., Park, Y. and Oh, S.H. (2000), "Designing robust sliding hyperplanes for parametric uncertain systems: a Riccati approach", *Automatica*, Vol. 36 No. 7, pp. 1041-1048.

Lau, K.C., Leung, E.Y.Y., Chiu, P.W.Y., Yam, Y., Lau, J.Y.W. and Poon, C.C.Y. (2016), "A flexible surgical robotic system for removal of earlystage gastrointestinal cancers by endoscopic submucosal dissection", *IEEE Transactions on Industrial Information*, Vol. 12 No. 6, pp. 2365-2374, doi: 10.1109/TII.2016.2576960.

Li, S., Yang, J., Chen, W.H. and Chen, X. (2013), *Disturbance Observer-Based Control: Methods and Applications*, CRC Press, Boca Raton, Florida, FL.

Lunardini, F., Casellato, C., d'Avella, A., Sanger, T.D. and Pedrocchi, A. (2016), "Robustness and reliability of synergy-based myocontrol of a multiple degree of freedom robotic arm", *IEEE Transactions on Neural Systems and Rehabilitation Engineering*, Vol. 24 No. 9, pp. 940-950.

Madonski, R., Ramírez-Neria, M., Gao, Z., Yang, J. and Li, S. (2019), "Attenuation of periodic disturbances via customized ADRC solution: a case of highly oscillatory 3DOF torsional plant", *2019 IEEE 8th Data Driven Control and Learning Systems Conference (DDCLS)*, Dali, China, pp. 1111-1116.

Martinez-Fonseca, N., Castaneda, L.A., Uranga, A., Luviano-Juarez, A. and Chairez, I. (2016), "Robust disturbance rejection control of a biped robotic system using high-order extended state observer", *ISA Transactions*, Vol. 62, pp. 276-286.

Mou, F., Wu, D. and Dong, Y. (2020), "Active disturbance rejection control with multilayer perceptron compensating network for robot systems", *Control Theory and Applications*, Vol. 37 No. 6, pp. 1397-1405.

Naik, P.R., Samantaray, J., Roy, B.K., *et al.* (2016), "2-DOF robot manipulator control using fuzzy PD control with SimMechanics and sliding mode control: a comparative study[C]", *International Conference on Energy*, IEEE.

Park, P., Choi, D.J. and Kong, S.G. (2007), "Output feedback variable structure control for linear systems with uncertainties and disturbances", *Automatica*, Vol. 43 No. 1, pp. 72-79.

Petit, F., Daasch, A. and Albu-Schaffer, A. (2015), "Backstepping control of variable stiffness robots", *IEEE Transactions on Control Systems Technology*, Vol. 23 No. 6, pp. 2195-2202.

Ren, T., Dong, Y., Wu, D. and Chen, K. (2018), "Collision detection and identification for robot manipulators based on extended state observer", *Control Engineering Practice*, Vol. 79, pp. 144-153, doi: 10.1016/j.conengprac.2018.07.004.

Sira-Ramirez, H., Luviano-Juárez, A., Ramírez-Neria, M. and Zurita-Bustamante, E.W. (2018), *Active Disturbance Rejection Control of Dynamic Systems: A Flatness Based Approach*, Butterworth-Heinemann, Oxford.

Su, Y., Muller, P.C. and Zheng, C. (2010), "Global asymptotic saturated PID control for robot manipulators", *IEEE Transactions on Control Systems Technology*, Vol. 18 No. 6, pp. 1280-1288.

Sun, J., Yang, J., Zheng, W. and Li, S. (2016), "GPIO-based robust control of nonlinear uncertain systems under time-varying disturbance with application to DC–DC converter", *IEEE Trans. Circuits Syst. II, Exp. Briefs*, Vol. 63 No. 11, pp. 1074-1078.

Talole, S.E., Kolhe, J.P. and Phadke, S.B. (2010), "Extended-state-observer-based control of flexible-joint system with experimental validation", *IEEE Transactions on Industrial Electronics*, Vol. 57 No. 4, pp. 1411-1419.

Van, M., Kang, H.J. and Suh, Y.S. (2013), "A novel neural second-order sliding mode observer for robust fault diagnosis in robot manipulators", *International Journal of Precision Engineering and Manufacturing*, Vol. 14 No. 3, pp. 397-406.

Van, M., Mavrovouniotis, M. and Ge, S.S. (2019), "An adaptive backstepping nonsingular fast terminal sliding mode control for robust fault tolerant control of robot manipulators", *IEEE Transactions on Systems, Man, and Cybernetics: Systems*, Vol. 49 No. 7, pp. 1448-1458, doi: 10.1109/tsmc.2017.2782246.

Wang, H., Li, S., Yang, J. and Zhou, X. (2016), "Continuous sliding mode control for permanent magnet synchronous motor speed regulation systems under time-varying disturbances", *Journal of Power Electron.*, Vol. 16 No. 4, pp. 1324-1335.

Wang, H., Pan, Y., Li, S. and Yu, H. (2019), "Robust sliding mode control for robots driven by compliant actuators", *IEEE Transactions on Control Systems Technology*, Vol. 27 No. 3, pp. 1259-1266, doi: 10.1109/tcst.2018.2799587.

Wen, C.C. and Cheng, C.C. (2008), "Designing of sliding surface for mismatched uncertain systems to achieve asymptotical stability", *Journal of the Franklin Institute*, Vol. 345 No. 8, pp. 926-941.

Xia, Y., Zhu, Z., Fu, M. and Wang, S. (2011), "Attitude tracking of rigid spacecraft with bounded disturbances", *IEEE Transactions on Industrial Electronics*, Vol. 58 No. 2, pp. 647-659.

Xue, W., Madonski, R., Lakomy, K., Gao, Z. and Huang, Y. (2017), "Add-on module of active disturbance rejection for set-point tracking of motion control systems", *IEEE Transactions on Industry Applications*, Vol. 53 No. 4, pp. 4028-4040.

Yang, J., Li, S. and Yu, X. (2013), "Sliding-mode control for systems with mismatched uncertainties via a disturbance observer", *IEEE Transactions on Industrial Electronics*, Vol. 60 No. 1, pp. 160-169, doi: 10.1109/tie.2012.2183841.

Yu, W. and Rosen, J. (2013), "Neural PID control of robot manipulators with application to an upper limb exoskeleton", *IEEE Trans. Cybern.*, Vol. 43 No. 2, pp. 673-684.

Yu, H., Shen, J.H., Joos, K.M. and Simaan, N. (2016), "Calibration and integration of B-mode optical coherence tomography for assistive control in robotic microsurgery", *IEEE/ASME Trans. Mechatronics*, Vol. 21 No. 6, pp. 2613-2623.

Zheng, Q. and Gao, Z. (2012), "An energy saving, factory-validated disturbance decoupling control design for extrusion processes", *World Congress on Intelligent Control and Automation*, pp. 2891-2896.

Zhou, W., Shao, S. and Gao, Z. (2009), "A stability study of the active disturbance rejection control problem by a singular perturbation approach", *Applied Mathematical Sciences*, Vol. 3 No. 10, pp. 491-508.

Further reading

Cao, Y. and Chen, X.B. (2014), "Disturbance-observer-based sliding-mode control for a 3-DOF nanopositioning stage", *IEEE/ASME Transactions on Mechatronics*, Vol. 19 No. 3, pp. 924-931, doi: 10.1109/tmech.2013.2262802.

Corresponding author
Fangli Mou can be contacted at: mfl18@mails.tsinghua.edu.cn